Accepted for presentation at the 13th International Symposium on Hazards, Prevention, and Mitigation of Industrial Hazards, (ISHPMIE), Braunschweig, Germany, July 27 – 31, 2020.
Paper #1010

Thermal ignition of n-hexane air mixtures by vertical cylinders

Silken Jones & Joseph Shepherd

Graduate Aerospace Laboratories, California Institute of Technology, Pasadena, CA, U.S.A
E-mail: *smjones@caltech.edu*

Abstract
An experimental study of thermal ignition of stoichiometric n-hexane and air mixtures by vertical cylinders is performed. Five cylinders were tested with surface areas ranging from 50 to 200 cm^2. Limited variation of igntion temperature with surface area was observed with ignition temperatures from 1019 to 1117 K; this is approximately 200 to 500 K higher than previous studies with similar surface areas. Quantitative temperature fields from the experiments were extracted via interferometry and the profile of the thermal layer agreed well with temperature results from numerical similarity solutions to the boundary layer equations. The ignition results are compared to relevant literature and the importance of a change in surface size versus a change in flow type is discussed.

Keywords: *combustion, thermal ignition, natural convection, aircraft safety*

1 Introduction

Accidental thermal ignition events caused by a hot surface represent a significant industrial safety hazard. It is important to understand the effect that a change in flow configuration or surface size has on ignition behavior. Current safety standards often do not account for such variation. For example, current Federal Aviation Administration (2018) regulations limit the maximum allowable temperature in a flammable leakage zone to 477 K (Federal Aviation Administration, 2018). This regulation does not consider the size or flow type of the hazard region. Flows can be internal or external, and subject to natural or forced convection.

Available literature does account for some variation in size or flow configuration. Previous studies by Kuchta et al. (1965) show a dependence of the ignition temperature on the surface area of the ignition source for surface areas from less than 1 cm^2 to 200 cm^2 for a variety of fuels including n-hexane. Surfaces less than 40 cm^2 in area are subject to external forced convection around a cylindrical rod or wire while the largest surfaces studied (greater than 40 cm^2) are heated vessels subject to internal natural convection. White (1967) studied thermal ignition by vessels filled with kerosene vapor mixtures subject to internal natural convection ranging from 250 to 6000 cm^2 in area. Ono et al. (1976) studied thermal ignition by vertical flat plates in propane, methane, ethaniol, and diethyl ether fuel mixtures with areas from 1.5 to 9 cm^2, subject to external natural convection. Smyth and Bryner (1997) investigated thermal ignition of many fuel mixtures including n-hexane by a flat plate 25 cm^2 in area, inclined at a number of angles to an external forced convection flow. Boettcher (2012) studied the effect of pressure, composition, and heating rate on ignition of n-hexane mixtures inside a vessel (380 cm^2) subject to internal natural convection flow. Melguizo-Gavilanes et al. (2016) studied thermal ignition by external natural convection of n-hexane mixtures over a glowplug (approximately a vertical cylinder) with a surface area of 1.5 cm^2. Boeck et al. (2017) studied thermal ignition of n-hexane by a small cylinder (3.14 cm^2) in horizontal and vertical orientations subject to external natural convection.

The purpose of the present work is to examine the effect of surface area on ignition by surfaces subject to external natural convection flows only. There is a particular scarcity of literature available for thermal ignition by external natural convection flows over surfaces larger than 10 cm^2. The surfaces investigated here are vertical cylinders ranging in size from 50 to 200 cm^2.

2 Experiments

2.1 Experimental Design

The surfaces studied are vertical cylinders made of stainless steel tubes with a wall thickness of 0.05 cm. The experiments are conducted in a cylindrical combustion vessel 30.4 cm in diameter by 66.0 cm tall filled with a reactive gas mixture. A cylinder is held in place inside the vessel with a copper support structure, which also provides a path for up to 375 A of current to flow to resistively heat the cylinder. A natural convection flow develops on the exterior as the cylinder heats up; the ends of the cylinder are sealed and the interior is filled with air. Water cooling is implemented at the ends of the cylinders to force a 298 K constant temperature in the support structure. This prevents the support structure from significant heating due to conduction and preserves the axisymmetry of the experiments. Axisymmetry is key for proper operation of the interferometer. The temperature of the cylinder is measured via two-color pyrometer and thermocouple, and quantitative temperature field measurements are taken via interferometer. Heating is achieved by applying constant current until within 10% of the preset temperature, at which point a temperature based feedback control system drives the cylinder to that temperature until ignition occurs or 300 seconds have elapsed. Figure 1 includes a schematic of the experimental setup.

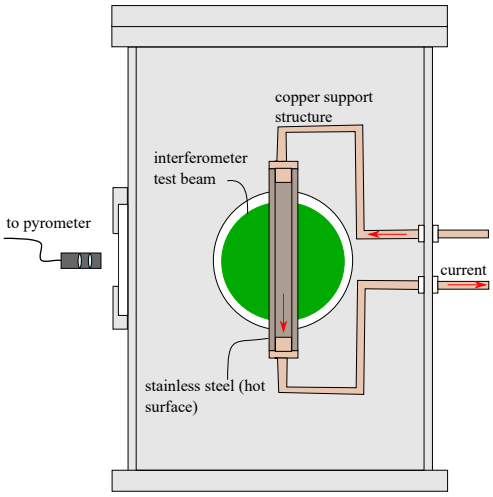

Fig. 1*: Experimental setup schematic, including combustion vessel, test cylinder, support structure, and diagnostics. Water cooling not shown.*

Five different cylinders are investigated in this work. Table 1 includes the measurements of all cylinders investigated.

Table 1*: Measurements of all five test cylinders*

Cylinder tag	Surface area, cm^2	Length, cm	Diameter, cm
50A	50	25.4	0.635
50C	50	12.7	1.27
75B	75	19.1	1.27
100A	100	25.4	1.27
100C	100	12.7	2.54
200A	200	25.4	2.54

2.2 Diagnostics

Two main diagnostics are used in these experiments. A two-color pyrometer takes non-contact surface temperature measurements of the cylinder, and an interferometer takes optical measurements of the temperature of the gas surrounding the cylinder.

2.2.1 Pyrometer

A two-color pyrometer takes non-contact measurements of surface temperature at a rate of 1 kHz. The benefit of the pyrometer is that it does not disturb the natural convection flow, enabling direct measurement of surface temperature at the location along the cylinder where ignition occurs.

The pyrometer collects light from the surface being measured. Light is split around 1800 nm by a longpass dichroic mirror. One narrow bandpass filter is used for each beam, one centered at 1700 nm and the other at 1940 nm to further filter the light. Finally, the light is projected onto a photodetector, one for each wavelength, which converts light intensity to a voltage reading. The ratio of bandpass-filtered radiation intensities, I_1/I_2, correlates with the surface temperature T_S. The advantage of a two color pyrometer is that it does not need to account for the value of surface emissivity when using the assumptions of gray-body emission, i.e. wavelength-independent emissivity, from the hot surface and narrow filter bandwidths. T_S is determined by equation 1:

$$T_S = \frac{A}{\ln(\frac{I_1}{I_2}) - B} \tag{1}$$

Constants A and B are determined by calibration with a blackbody radiation source (Process Sensors BBS1200). The spot size of the pyrometer is determined during calibration to be approximately 0.32 cm in diameter.

Initial characterization of the cylinders shows that a large central portion of a cylinder reaches a uniform high temperature. Approximately the last two centimeters at each end of a cylinder are cooler due to conduction to the water cooled end. To test the pyrometer operation immediately before ignition testing, a cylinder is heated up in air and allowed to oxidize until a thick oxide layer develops and subsequent oxidation is very slow. During this oxidation period, pyrometer measurements of the central hot region of the cylinder are checked against thermocouple measurements taken in the same region. Additionally, a thermocouple is placed at the top of the cylinder in the cooler edge region. This is above the location where ignition occurs and should not disturb natural convection flow development in the ignition region. Heating tests are performed to construct a polynomial fit by which the temperature of the central hot region can be extrapolated from the temperature reading of the top thermocouple. The central thermocouple is removed before ignition testing, while the top thermocouple remains to provide a double check for the pyrometer reading. Figure 2 shows a schematic of this situation.

2.2.2 Interferometer

Interferometry has a long history as a technique to make gas temperature measurements. Coronel et al. (2018) presents a detailed account of the exact postprocessing techniques used in our laboratory to extract temperature field measurements of a gas from interferometry. A new interferometer design is implemented for this set of experiments and is briefly described here.

The surfaces under investigation in this work are much larger in size than those in Coronel et al. (2018) so an interferometer with a much larger test beam is constructed. The design chosen is a modified Mach-Zehnder interferometer, with the test beam expanded to 101.6 mm diameter at the focal plane and the reference beam transmitted through an optical fiber. Figure 3 shows a schematic of the

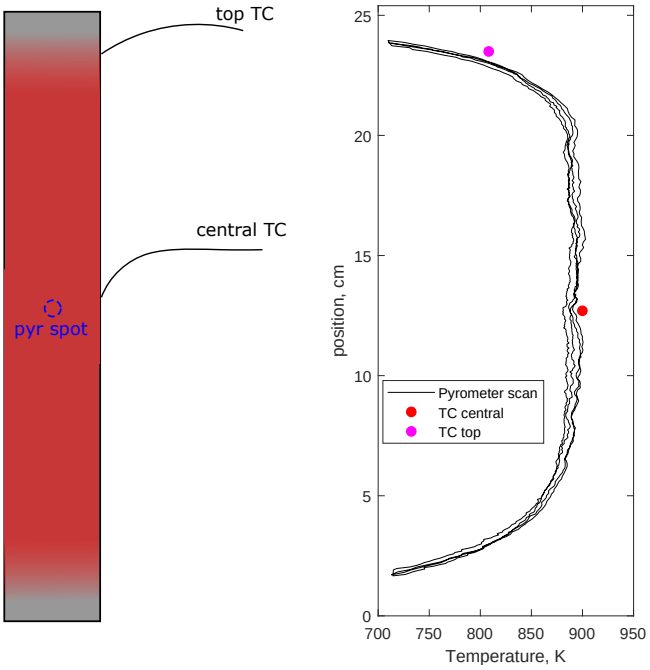

Fig. 2*: (Left) Placement of thermocouples and pyrometer during heating tests. The central hot region is indicated in red, fading to the cooler edge region in gray. (Right) Temperature distribution along cylinder length from cylinder characterization compared with thermocouple measurements.*

interferometer.

532 nm light from a Coherent Sapphire laser at emerges at the laser head with a 0.7 mm diameter. It is expanded once by a 5X beam expander to a 3.5 mm diameter. The light is then split by a 50:50 unpolarized cubic beamsplitter into a test beam and a reference beam. The test beam is expanded again by a factor of 5X to 17.5 mm diameter and a focusing lens and a concave mirror are used to collimate the light at a diameter of 101.6 mm. This matches the aperture of the windows on the combustion vessel and maximizes the amount of information that the interferometer can collect at the focal plane. After the test beam passes through the combustion vessel it is condensed to a 17.5 mm beam diameter by an identical concave mirror and focusing lens pair. It then passes through the second beamsplitter to recombine with the reference beam.

After splitting from the test beam the reference beam couples into a single mode polarization preserving fiber with the use of an 18 mm focal length collimation package. The collimation package is compatible with the 3.5 mm diameter of the test beam. The fiber is routed to the other side of the interferometer. An identical collimation package is used at the fiber output to return the reference beam to a 3.5 mm diameter. A third 5X beam expander is used to match the reference beam diameter to the test beam. The two beams recombine at the second beam splitter. The combined beams pass through a final focusing lens to ensure the the focal plane coincides with the center of the test cylinder. A Phantom V711 camera is used to record the interferometer at frame rates in excess of 10,000 fps. The method described by Coronel et al. (2018) is used to post process the recorded interference patterns.

The new interferometer design was checked for validity by placing a well-characterized hot surface (Autolite glowplug from Boettcher (2012) and Melguizo-Gavilanes et al. (2016)) in the focal plane. The surface was heated in nitrogen while interferometer recordings were taken, and the post-processed temperature fields were compared against previous temperature field results validated for the glowplug heating configuration. Temperature fields extracted from this new interferometer compared very well with previous results, indicating the accuracy of the new interferometer.

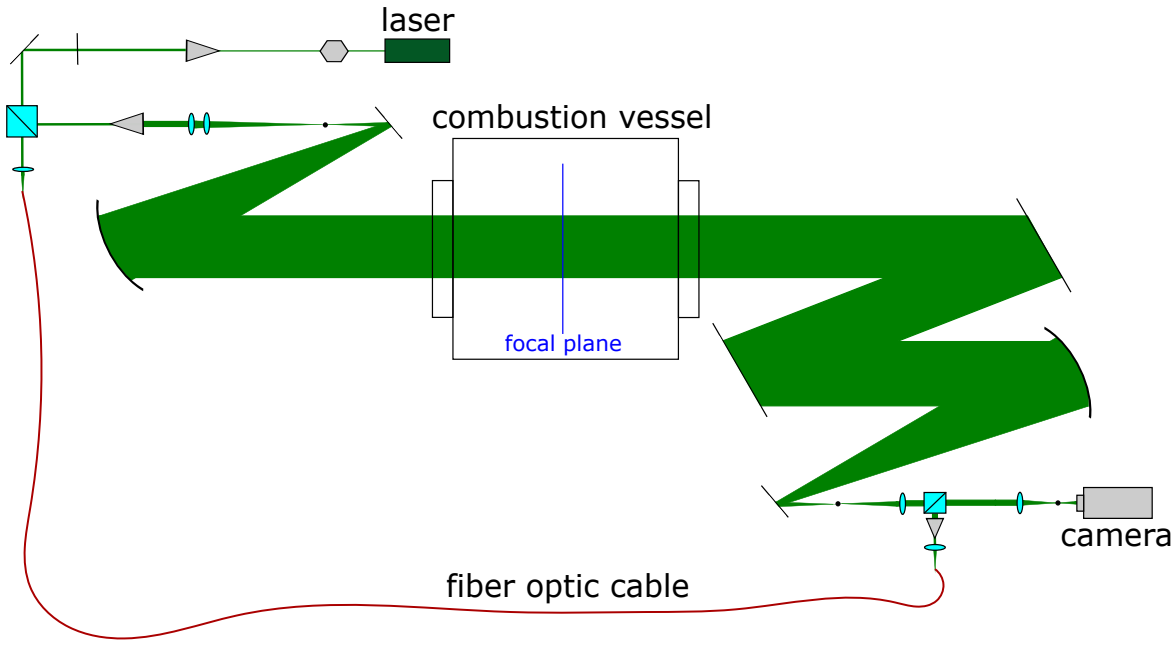

***Fig. 3**: Schematic of Mach-Zehnder interferometer with fiber optic reference beam. Focal plane of interferometer is inside the test section/combustion vessel and is shown in dark blue.*

3 Numerical methods

To gain an understanding of how the natural convection flow develops, a suitable numerical method is implemented. The goal for this numerical method is to make predictions of the thermal layer development that can then be compared with experimental tempertature fields from interferometry.

The similarity solution developed by Cairnie and Harrison (1982) presents a numerical method for solving the boundary layer equations over a vertical flat plate with a high temperature difference between wall and ambient conditions. Gas properties such as density, viscosity, heat capacity, and thermal conductivity are highly variable due to the large temperature difference. The dependency of these properties on temperature is accounted for in the numerical method (Cairnie and Harrison, 1982). Capturing this dependency is key to getting accurate results for large temperature differences. The implementation in MATLAB is checked for validity by using the conditions presented in Cairnie and Harrison (1982) and comparing the output to their original results. The numerical method is subsequently used to predict development of natural convection over flat plates of the same length as the cylinders studied experimentally.

4 Results and discussion

Experiments are conducted as described in Section 2.1 with a stoichiometric n-hexane and air mixture. N-hexane is chosen as a fuel because it is a simple surrogate for aviation kerosene and because of its legacy use within the laboratory which enables direct comparison with previous work. Boeck et al. (2017) show little variation in ignition temperature of n-hexane mixtures with composition up to the flammability limits so only one mixture composition is investigated in this work. More than 20 tests are conducted for each cylinder with the exception of 100C. It is important to note that the power supply used (Magna Power XR5-375/208) is not powerful enough to heat cylinder 100C to ignition temperatures. The maximum temperature achieved over five tests of 100C is 1013 K and no ignition is observed.

The independent variable in these tests is surface temperature, T_S, at trigger time. The trigger is caused by a pressure spike in tests with ignition and the time to ignition ranges from approximately 30 to 260

s. The triggering is done manually after 300 seconds of test time for non ignition tests. The test time is limited to 300 s because preliminary tests with longer test times did not exhibit change in behavior. The dependent variable is a binary outcome of 0 or 1 representing a non-ignition and ignition result respectively. The data pairs of (T_S, binary ignition variable) are plotted in Figure 4 for cylinders 50A and 50C as examples. These data pairs can also be used to generate a logistic regression model for the probability of achieving ignition as a function of T_S. The temperature set points are chosen to span the range of interest such that both ignition and non ignition events will be observed to provide both the number and quality of data points to enable useful statistics from the logistic regression. Bane et al. (2011) discuss set point picking methods and provide a detailed description of the procedure used to generate the probability model. This probability function is represented in Figure 4 by a solid black line.

4.1 Ignition temperatures and overlap behavior

Table 2 shows the ignition temperature (T_S at which there is a 50% probability of ignition) for all cylinders investigated. It also indicates if a cylinder demonstrated any sign of overlap behavior. Overlap occurs when there are T_S at which both ignition and non ignition results are observed. Overlap can be seen first in the raw data points in Fig. 4 (left). There is a non ignition case with higher T_S than two of the lowest temperature ignition cases. Overlap is also indicated by a more gradual rise in the probability function and indicates increasing variability in the results. Cylinders 50A, 75B, 100A and 200A demonstrate overlap behavior, while no overlap is seen in cylinder 50C. Overlap occurs with longer cylinder lengths (19.1 and 25.4 cm), indicating that there is more scatter in ignition results with longer cylinders. Overlap can also be examined in the context of aspect ratio; cylinder 50C exhibits no overlap behavior with an aspect ratio of 0.1 while 200A has the same aspect ratio and does demonstrate overlap behavior. Consequently, cylinder length is a more appropriate variable to indicate overlap behavior versus aspect ratio. Future work planned with a wider range of cylinder lengths and aspect ratios will further inform the role of these variables in overlap behavior.

The uncertainty in the ignition temperatures can be quantified in two ways. The first is to look at the width of the 95% confidence limits on the probability function at fifty percent probability of ignition. This produces an uncertainty of $\pm$8 K for cylinder 50A, $\pm$5 K for cylinder 75B, $\pm$6 K for cylinder 100A, and $\pm$5 K for cylinder 200A. The confidence limits cannot be calculated for cylinders that do not exhibit overlap behavior. The other way to quantify uncertainty is to use the uncertainty of pyrometer measurements which is calculated during calibration to be $\pm$ 30 K. The pyrometer uncertainty is larger than that from the confidence limits on the probability function and applies to all cylinders investigated. The pyrometer uncertainty is therefore used in all subsequent discussion of uncertainty on ignition temperatures.

***Table 2**: Ignition Temperature Results*

Cylinder tag	T_{ign}, K	L, cm	Aspect Ratio, D/L	Overlap?
50A	1085	25.4	0.025	1
50C	1117	12.7	0.1	0
75B	1078	19.1	0.066	1
100A	1055	25.4	0.05	1
100C	1013 (max T, no ign)	12.7	0.2	–
200A	1019	25.4	0.1	1

4.2 Gas temperature fields

The numerical results from Section 3 are presented in Figure 5 for a plate 25.4 cm long. Results for a shorter plate can be obtained by truncating the numerical results at the desired total height of the plate.

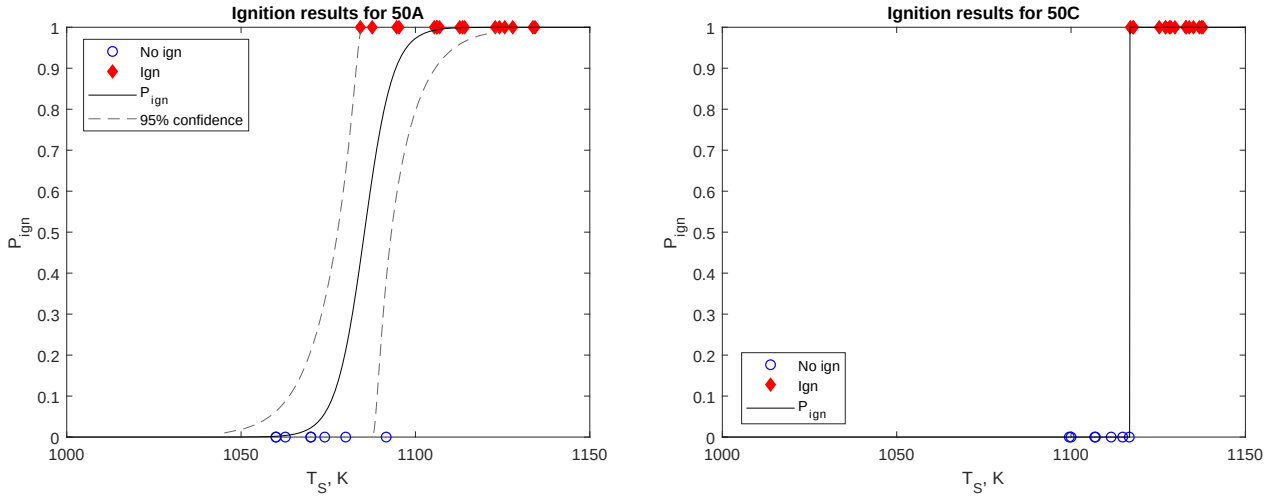

***Fig. 4**: Left: Ignition data for cylinder 50A. Test results show overlap in temperatures for ignition (red filled diamonds) and non-ignition (empty blue circles) results. Right: Ignition data for cylinder 50C. Test results show no overlap in temperatures for ignition and non-ignition results. The black line shows the probability of ignition as a function of temperature and the gray dashed lines show the 95% confidence limits on the probability function where applicable.*

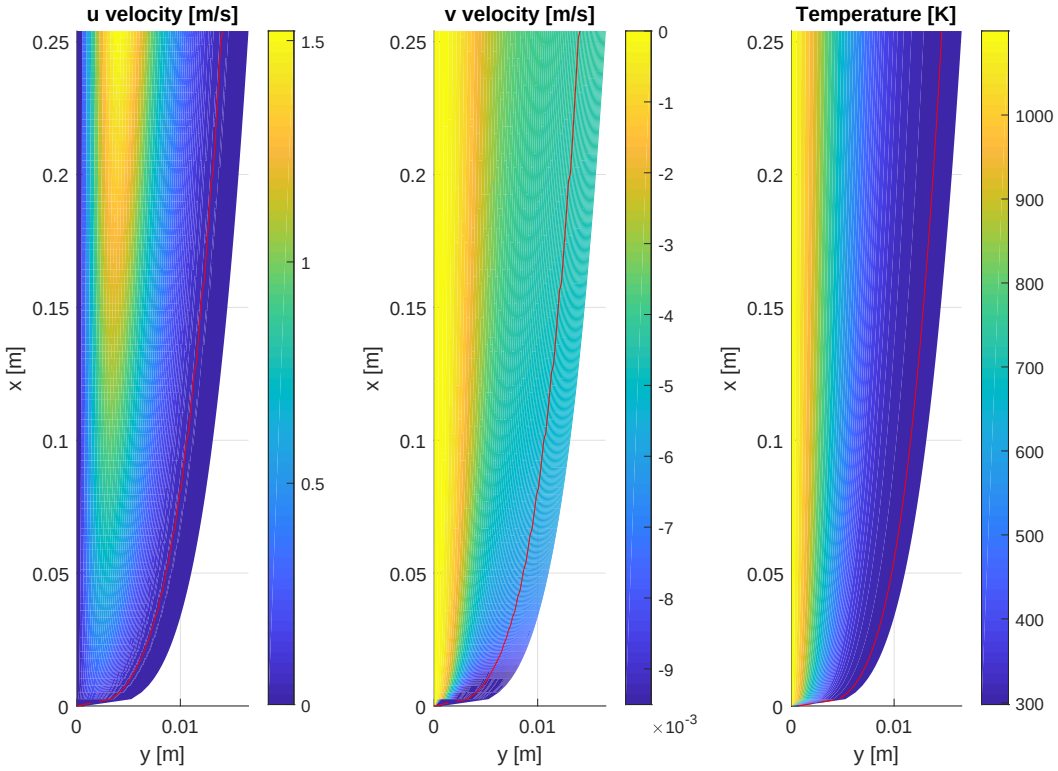

***Fig. 5**: Results from numerical method presented in Section 3. Fields of velocity parallel to wall (u), velocity perpendicular to wall (v), and temperature (T) are presented. The red line shows where numerical results are within 1% of ambient conditions.*

Velocity fields parallel and perpendicular to the wall and temperature fields are presented. The wall parallel velocity takes the expected structure for a natural convection flow: no-slip creates a velocity of zero next to the wall. Buoyancy forces increase the velocity as distance from the wall increases, reaching a maximum before velocity drops again to zero at the edge of the momentum layer to match

ambient conditions. Similarly, wall perpendicular velocity appears as expected for a natural convection flow. The velocity is largest and negative at the leading edge of the cylinder as gas is entrained into the natural convection flow. The entrainment effect becomes less pronounced along the outer edge of the momentum layer as distance from the leading edge increases. The perpendicular velocity next to the wall is zero. Temperature results show the gas matches wall temperature immediately next to the surface and then gas temperature drops off exponentially until ambient temperature is matched at the edge of the thermal layer. Additionally, the width of the thermal layer increases very quickly in approximately the first centimeter along the plate, after which there is a much more gradual increase in the width of the thermal layer as the distance from the leading edge increases.

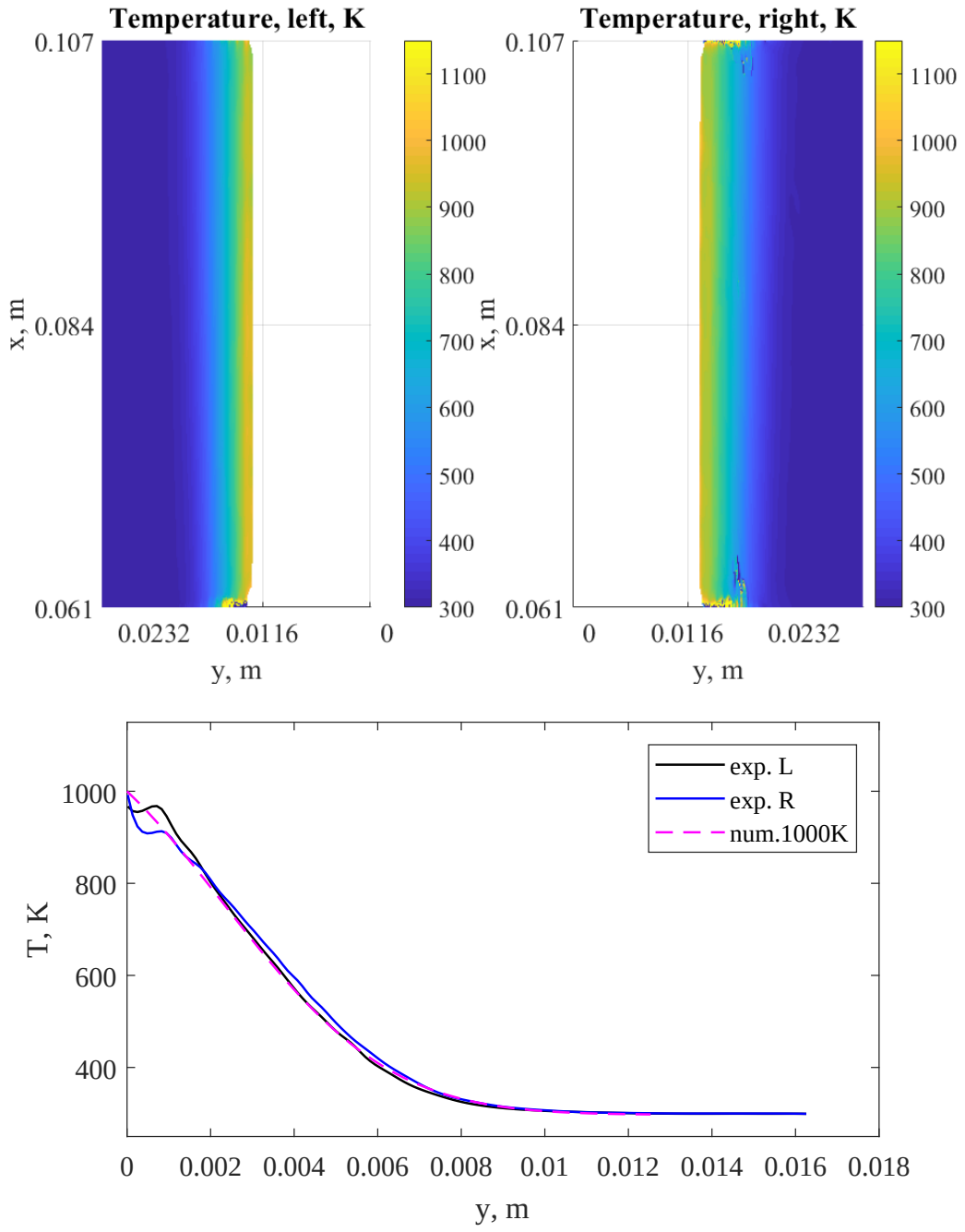

***Fig. 6**: Processed interferometer results for cylinder 100C in pure N_2, T_S = 1001 K. Top: experimental temperature fields from interferometery for both sides of cylinder averaged over 100 s of steady-state T_s. Bottom: Comparison of thermal layer profiles at 8.4 cm along cylinder for left and right sides of experimental temperature fields as well as for numerical results.*

These numerical results can be compared directly with experimental results. Fig. 6 shows the experimental temperature fields for cylinder 100C in pure nitrogen with a wall temperature of 1000 K. It also compares the thermal layer profile on both sides of the cylinder with the numerical results 8.4 cm from the leading edge. The experimental temperature fields are symmetrical, indicating good axisymmetry in the experiments. There are artifacts visible 0.001 m from surface; these are due to errors in the postprocessing methods including errors from subpixel inaccuracies in picking the centerline of the surface which results in errors accumulating towards the center of the processed image. Despite these artefacts from postprocessing, comparing the thermal layer profile for both sides of the cylinder with the numerical results shows that the numerical method accurately predicts the thermal layer observed experimentally with less than 6% error.

The agreement between both sides of the post-processed interferometer results and the numerical results indicates that experimental temperature fields are accurately reconstructed, and that the numerical method from Section 3 is useful for predicting the natural convection flow. There are some limitations to the numerical method presented in Section 3. First, the similarity solution developed by Cairnie and Harrison (1982) is developed for flat plates and the experiments are conducted on vertical cylinders. The numerical method does not account for effects of curvature of the surface. Approximating a vertical cylinder as a vertical flat plate with less than 5% error is assumed valid so long as Equation 2 holds.

$$\frac{D}{L} \geq \frac{35}{Gr_L^{0.25}} \tag{2}$$

Where D is the diameter of the cylinder, L is the height of the cylinder, and Gr_L is the Grashof number based on the height of the cylinder. This approximation comes from Sparrow and Gregg (1956). None of the cylinders satisfy the inequality, but for cylinder 100C the right and left hand sides of Equation 2 are within the same order of magnitude. Since there is an excellent comparison with the numerical prediction of the thermal layer in this case we conclude that this cylinder can still be approximated as a flat plate with reasonable accuracy despite not meeting the limit posed by Sparrow and Gregg (1956). Additionally, the numerical method only considers inert gases; there is no consideration of reaction effects. Despite these limitations, the numerical results for temperature compare well with experimental temperature fields from interferometry prior to the onset of significant visible reaction, as shown by Fig. 6.

4.3 Comparison with literature results

The ignition results from Section 4.1 can also be compared with results from the literature. First, the results are compared with those from Kuchta et al. (1965) for internal natural convection of n-hexane mixtures with similar surface areas, as show in Fig. 7. The mixture composition of the data points from Kuchta shown in Fig. 7 is not reported in the original text but the range of mixture compositions investigated varied from 0.05 to 0.5 fuel-air weight ratio with little effect of composition. There is a significant change in ignition temperature between internal and external natural convection flows with similar surface areas. The ignition temperatures for external natural convection flows investigated here are approximately 200 to 500 K higher than the ignition temperatures for internal natural convection (Kuchta et al., 1965).

This can be explained by the difference in confinement between these two flow configurations. An internal natural convection flow is confined inside a heated vessel and the reactive mixture continuously recirculates within that vessel, getting exposed to the heated surface many times. The significant confinement and recirculation causes a long residence time. Long residence times generally lead to lower ignition temperatures as fuel is able to decompose and slower low-temperature chemistry can occur. For external natural convection flows in unconfined geometries the reactive mixture is only exposed to the hot surface once as it moves through the thermal layer. The gas does not recirculate and the

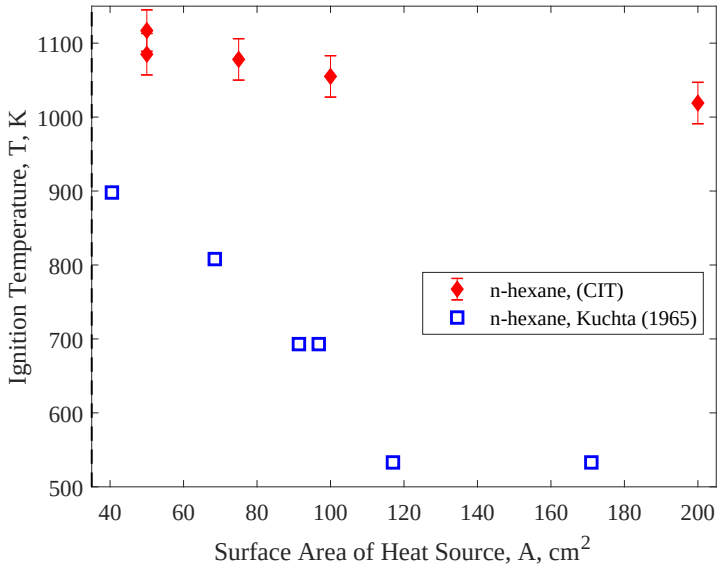

***Fig. 7**: Ignition results from this work (red filled diamonds) compared with those from Kuchta (1965) (blue empty squares) for a similar range of surface areas.*

residence time is shorter. If the external flow is confined in some manner (e.g. inside a vessel), it is possible the flow recirculates and thus increases the residence time. In such situations it is important to understand if there is recirculation of the flow.

Because the hot cylinder in the present study is confined within a closed vessel, there is the potential for recirculation of gas through the thermal layer. The natural convection around the cylinder acts a pump with cold gas entering from the bottom, accelerating upward and exiting the top of the thermal layer. The total mass flow rate induced by this process can be estimated from the model of natural convection presented in Section 3. Using the numerical results presented in Section 4.2, the wall parallel velocity and density are numerically integrated to estimate the mass flow rate. Wall perpendicular velocity is neglected as it is two orders of magnitude smaller than wall parallel velocity.

$$\dot{m} = \int_V \rho u dV = \int_0^L \int_0^{2\pi} \int_{R_c}^{R'} \rho(r,z) u(r,z) r dr d\theta dz \tag{3}$$

Where L is the length of the cylinder, R_c is the radius of the cylinder, and R' is the outer radius of the flow as determined by the point at which conditions are within one percent of ambient values. The shortest estimated recirculation time, estimated as $M/\dot{m}$ where M is the total mass of gas in the vessel, is 460 seconds and corresponds to cylinder 200A. This is 50% more than the test time of the experiments. Therefore it is reasonable to assume there is no significant recirculation in these experiments and any given portion of the reactive mixture is heated only once.

Comparisons can also be made with the wider body of literature. Starting with results on external natural convection, Melguizo-Gavilanes et al. (2016) report ignition temperatures of n-hexane with an equivalence ratio of 0.9 at 1275 $\pm$ 45 K for a glowplug (approximately a vertical cylinder) with 1.5 cm^2 surface area. Boeck et al. (2017) report ignition temperatures of 1270 K for stoichiometric n-hexane air mixtures for a vertical cylinder 3.14 cm^2 in area and Ono et al. (1976) report an ignition temperature of approximately 1250K for stoichimetric propane-air and vertical plates 9 cm^2 in area. Data from all cited studies are compared against results from this work in Fig. 8. Two conclusions are drawn when literature data is compared with the results found in this work. Ignition temperatures for external natural convection are consistently much higher than ignition temperatures for internal

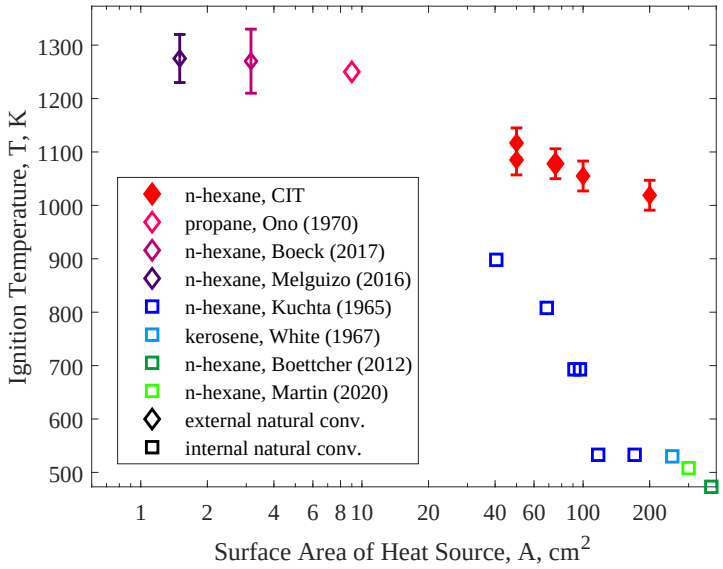

***Fig. 8**: Ignition results from this work (red filled diamonds) compared with results from literature. External natural convection represented by diamonds and internal natural convection represented by squares.*

natural convection flows. Additionally, there is a significant difference in the trend of ignition temperature with surface area. Kuchta et al. (1965) report ignition temperature dropping from 898 K at 40.5 cm^2 to 533 K at 171 cm^2 which amounts to a 365 K decrease in ignition temperature over 130 cm^2 of area change. For a similar area change the ignition temperature of the cylinders drops from 1117 K at 50 cm^2 to 1019 K at 200 cm^2. This is a difference of 98 K over a 150 cm^2 area change and shows a much more modest depended of ignition temperature on surface area in comparison to Kuchta et al. (1965).

Additional literature on thermal ignition from internal natural convection gives points of comparison for the results of Kuchta et al. (1965). White (1967) reports ignition temperatures of 530 K for a vessel approximately 250 cm^2 in area with an air-fuel ratio from 0.85 to 40 for kerosene-air mixtures. Boettcher (2012) reports ignition temperatures of 473 K for a 380 cm^2 vessel with n-hexane fuel at an equivalence ratio of 1.2. Martin and Shepherd (2020) followed the autoignition testing procedure prescribed by ASTM E659 (ASTM International, 2015) and found an ignition temperature of 508 $\pm$ 3 K for hexane in a 300 cm^2 vessel. These results further demonstrate the large difference in ignition temperatures between internal and external natural convection flows. This indicates that a change from internal to external flow has much more impact on ignition temperature than a change in surface area for the range investigated here.

5 Conclusions

Thermal ignition of stoichiometric n-hexane and air mixtures by vertical cylinders from 50 to 200 cm^2 is investigated experimentally. Five out of six of the tested cylinder geometries achieve ignition. Ignition thresholds are found to range from 1019 to 1117 $\pm$ 30 K. Surface temperatures at which both ignition and non ignition results are observed, e.g. overlap behavior, are found for cylinders with longer lengths (19.1 to 25.4 cm) but are not observed with a cylinder length of 12.7 cm. This indicates that a longer cylinder and thus a longer residence time leads to more scatter in ignition results.

For inert mixtures, a simple similarity-type solution accurately predicts the thermal layer formed by natural convection over a vertical cylinder. Temperature fields from interferometry compare well with

numerical results from a similarity solution adapted from Cairnie and Harrison (1982). This indicates that the similarity solution is useful for predicting momentum and thermal layers as long as the right and left hand sides of Equation 2 are of the same order of magnitude.

Finally, cylinder ignition results are compared to published values obtained by previous researchers. The ignition temperatures from this work are overall consistent with ignition temperatures for other external natural convection flows. Examination of ignition temperature data from external natural convection flows shows a modest decrease in ignition temperature as surface area increases for a total of 220 K decrease between 1275 K at 1.5 cm^2 and 1019 K at 200 cm^2. The present study demonstrates that external natural convection over hot surfaces results in ignition temperatures which are significantly higher and much less dependent on surface area than previous studies that used natural convection inside heated vessels.

Acknowledgements

This work was carried out in the Explosion Dynamics Laboratory of the California Institute of Technology, and was supported by The Boeing Company through a Strategic Research and Development Relationship Agreement CT-BA-GTA-1. The authors gratefully acknowledge the contributions of Esmir Mesic on initial characterization of the cylinders.

References

ASTM International (2015). *ASTM E659-15, Standard Test Method for Autoignition Temperature of Chemicals*.

Bane, S., Shepherd, J., Kwon, E., Day, A. (2011). *Statistical analysis of electrostatic spark ignition of lean $H_2/O_2/Ar$ mixtures.* International Journal of Hydrogen Energy, 36:2344–2350.

Boeck, L., Meijers, M., Kink, A., Mével, R., Shepherd, J. E. (2017). *Ignition of fuel-air mixtures from a hot circular cylinder*. Combustion and Flame, 185:265–277.

Boettcher, P. (2012). *Thermal Ignition*. Ph.D. thesis, California Institute of Technology.

Cairnie, L. R., Harrison, A. J. (1982). *Natural Convection Adjacent to a Vertical Isothermal Hot Plate with a High Surface to Ambient Temperature Difference*. International Journal of Heat and Mass Transfer, 25(7):925–934.

Coronel, S., Melguizo-Gavilanes, J., Jones, S., Shepherd, J. (2018). *Temperature field measurements of thermal boundary layer and wake of moving hot spheres using interferometry*. Experimental Fluid and Thermal Science, 90:76–83.

Federal Aviation Administration (2018). *Advisory circular 25.981-1D*.

Kuchta, J., Bartkowiak, A., Zabetakis, M. (1965). *Hot surface ignition temperatures of hydrocarbon fuel vapor-air mixtures*. Journal of Chemical Engineering Data, 10(3):282–288.

Martin, C., Shepherd, J. (2020). *Low temperature autoignition of jet a and surrogate jet fuels*. 13th International Symposium on Hazards, Prevention, and Mitigation of Industrial Explosions.

Melguizo-Gavilanes, J., Nove-Josserand, A., Coronel, S., Mevel, R., Shepherd, J. E. (2016). *Hot surface ignition of n-hexane mixtures using simplified kinetics*. Combustion Science and Technology, 188(11–12):2060–2076.

Ono, S., Kawano, H., Niho, H., Fukuyama, G. (1976). *Ignition in a free convection from vertical hot plate*. Bulletin of the JSME-Japan Society of Mechanical Engineers, 19(132):676–683.

Smyth, K., Bryner, N. (1997). *Short-duration autoignition temperature measurements for hydrocarbon fuels near heated metal surfaces*. Combustion Science and Technology, 126(16):225–253.

Sparrow, E. M., Gregg, J. L. (1956). *Laminar-Free-Convection Heat Transfer From the Outer Surface of a Vertical Circular Cylinder*. Transactions of the ASME, 78:1823–1829.

White, R. (1967). *Spontaneous ignition of kerosene/avtur/vapour - the effect of the ratio, vessel surface area to volume (effect of vessel surface area on minimum spontaneous ignition temperature of kerosene)*. Technical Report 67107, Royal Aircraft Establishment.